Cement and Concrete Composites 163 (2025) 106222

Contents lists available at ScienceDirect

Cement and Concrete Composites

journal homepage: www.elsevier.com/locate/cemconcomp

Carbonation induced changes in the mechanical performance, water and chloride permeability of Portland cement-slag-limestone ternary cement concretes

Moro Sabtiwu [a], Yuvaraj Dhandapani [a], Michal Drewniok [a], Samuel Adu-Amankwah [a,b], Susan A. Bernal [c,*]

[a] School of Civil Engineering, University of Leeds, Woodhouse Lane, Leeds, LS2 9JT, United Kingdom
[b] School of Engineering and Applied Science, Aston University, Birmingham, B4 7ET, United Kingdom
[c] Department of Architecture and Civil Engineering, University of Bath, Claverton Down, Bath, BA2 7AY, United Kingdom

ARTICLE INFO

Keywords:
CEM VI
Limestone ternary cements
Ground granulated blast furnace slag
Carbonation
Sorptivity
Chloride ingress

ABSTRACT

Carbonation and chloride-induced deterioration of reinforced concrete can cause infrastructure damage and potential collapse. This study evaluated the impact of carbonation on compressive strength, dimensional stability, water and chloride permeability of concretes made with ternary slag cement containing 10 or 20 wt.% limestone, compared to ground granulated blast furnace slag (GGBFS) blended cement or CEM I. The carbonation rates of binary and ternary concretes were higher than those of CEM I concrete. The existing equation correlating natural and accelerated carbonation coefficients holds for the concretes evaluated and the selected carbonation exposure condition studied. The carbonation depths estimated adopting this correlation are within the limits of the cover depths recommended by the BS 8500–1:2023 for concretes for a 50 years' service life, when exposed to exposure classes XC3/XC4. Despite the higher carbonation rates, water and chloride permeability of the carbonated ternary and binary slag cement concretes were significantly lower than those of a CEM I equivalent. No clear correlation was identified between compressive strength, porosity, bulk conductivity, water sorption coefficient and carbonation rate. Each of these properties alone did not give a good indication of the overall durability performance of binary or ternary concretes. The results demonstrate that 10 % limestone addition has no adverse effect on carbonation resistance of composite cement concrete. Therefore, it is demonstrated that partial replacement of GGBFS by limestone is a practical and technically sound solution for producing concrete with a reduced clinker content and comparable durability to CEM I or binary GGBFS concretes.

1. Introduction

Climate change poses a great threat to the built environment, as the longevity and resilience of concrete infrastructure can be compromised due to extreme weather changes, along with increased CO_2 concentrations in the air. The chemical reaction between the cementitious matrix of a concrete, and the CO_2 diffusing into the material is referred to as carbonation. Corrosion of steel reinforcement in structural concrete can be triggered by the carbonation of the binding phase (causing reductions in pH and pore structure alterations) and/or the penetration of chlorides through the carbonated concrete cover layer. In the case of concretes produced with cement replacements or supplementary cementitious materials (SCMs), it is known that carbonation can lead to increased porosity and reduction in strength [1–3]. There is an increasing interest in the adoption of composite cement comprising blast furnace slag-limestone [4,5] and calcined clay-limestone blends [6,7], for example, cements referred in the European standards as CEM VI (S-L)/CEM VI(S-LL). Studies on their phase assemblage [5], pore structure development [4,8,9], chloride resistance [10], and freeze-thaw resistance [11] are widely reported in the literature. However, there are limited studies evaluating carbonation resistance, and carbonation-induced changes to concrete performance. Therefore, it is critical to assess how carbonation might impact the overall durability of binary granulated blast furnace slag (GGBFS) cement concrete, and limestone ternary equivalent, particularly chloride permeability.

The correlation between carbonation performance and cementitious

* Corresponding author.
E-mail address: sbl30@bath.ac.uk (S.A. Bernal).

https://doi.org/10.1016/j.cemconcomp.2025.106222
Received 18 February 2025; Received in revised form 11 June 2025; Accepted 6 July 2025
Available online 9 July 2025

material properties has been a subject of extensive research [12–14], this to determine how the mechanical strength properties is affected by the intrinsic matrix features (such as buffer capacity and pore structure) for a given cement type and mix design formulation. Carbonation is both a chemically and a diffusion-controlled deterioration mechanism, and consequently, compressive strength values alone are not sufficient to capture the complex changes that might be taking place in the material as carbonation progresses. While it is well accepted that compressive strength is not a suitable descriptor of the carbonation resistance of concrete, some studies have shown that concretes with higher compressive strength present lower carbonation rates due to refined pore structures. For example, Leeman and Moro [12], and Sulapha et al. [15] reported correlations between compressive strength and carbonation coefficients for binary GGBFS blended concretes; however, Shah and Bishnoi [16] identified no correlation between these properties. Nonetheless, there seems to be a consensus regarding the influence of the CO_2 buffer capacity (i.e., related to the total alkali content and reserve alkalinity) on the carbonation resistance of slag blended concrete. On the relationship between porosity and carbonation coefficient, Shah and Bishnoi [16] and Sulapha et al. [15] reported no dependency on binary GGBFS systems or other ternary SCM systems. A gap in such studies is the lack of clarity on the understanding of the implications of pore structure changes on transport properties arising from carbonation-induced dimensional stability and/or microcracking in SCM concrete systems [1]. Although some studies have explored carbonation mechanisms in composite cements in terms of its influences on phase assemblage alterations and pore structure modifications [16–18], there are limited studies characterising the impact of carbonation on water and chloride penetration, which would influence the long-term performance. Bridging this knowledge gap is critical to predict the long-term performance, particularly for ternary slag-limestone cements which have not been extensively utilised in real practice [19].

Recent evidence has demonstrated that carbonation alone does not lead to corrosion of steel [20]. Other factors such as pore structure and moisture content at the steel-concrete-interface play a key role in destabilizing the passivation layer formed in the steel surface. This has been addressed in some standards by increasing concrete cover depth [21,22], aimed at delaying the progression of carbonation/pH loss near the steel reinforcement. However, it remains largely unknown how carbonation progress will modify the overall permeability properties of concrete produced with different cement types, and its influence on the ingress of other deleterious species, such as chlorides, as it is unlikely that under a realistic in-service environment, the material will be exposed to only one durability stress. It is also worth noting that reports on the carbonation performance of concretes made with CEM VI are scanty, and their longer-term carbonation performance has not been extensively evaluated. This is consistent with the fact that such cement types were only included in European standards in the last years and, in the case of the UK, were only included in 2023.

The impact of carbonation on the concrete transport properties has received some attention in literature mostly for CEM I and binary systems or ternary systems where Portland cement is replaced with GGBFS in addition to other SCMs, but not with limestone. Even though multi-component cements containing slags and up to 20 wt% limestone powder have been standardised (BS 8500–2:2023 [23] and EN 197–5:2021 [24]), limited records exist on their durability performance upon carbonation. Hren et al. [25] investigated the impact of exposure to 3 % CO_2 accelerated carbonation of 28 days cured mortars containing GGBFS (CEM III/B (S) 32.5 N – LH/SR) relative to CEM I, on the ingress of chlorides (52 weeks 3.5 % NaCl ponding). Their chloride profiling results showed that accelerated carbonation resulted in 30 % increase in free chloride, but 21 % reduction under natural carbonation in GGBFS-blended materials relative to CEM I. Similarly, Li et al. [26] subjected 90-days moist cured concretes made with CEM I, and ternary slag-fly-ash concretes to 90 days of natural and accelerated (20 % CO_2) carbonation followed by chloride immersion (15 g/L NaCl) for 35 days. It was shown that near the carbonation front, the free chloride concentration increased under accelerated exposure compared to natural carbonation, but lower in the SCM containing concretes in all cases, plausibly due to binding. Towards the boundary between the carbonated and the non-carbonated area, the chloride concentrations decreased slightly, and then progressively reduced further away from the carbonation front. It was established that the net change in apparent chloride diffusivity under accelerated and natural carbonation was lower in blended systems relative to CEM I, and it was hypothesised that this phenomenon is independent of increasing carbonation depth. Limestone in the ternary cement can modify the phase assemblages and pore structure compared to binary slag cements. Consequently, the carbonation resistance and post-carbonation chloride ingress may be altered.

In the current study, four concrete mixes, including CEM I, blended slag cements with and without limestone additions, were produced, and their carbonation resistance was determined under controlled natural and accelerated conditions. Changes in water and chloride permeability were subsequently assessed on carbonated concrete. The dimensional stability during carbonation and residual strength were also evaluated.

2. Experimental methods

2.1. Materials

In this study similar materials to those used in a previous study by the authors [27] were adopted. Commercial CEM I 52.5N and granulated blast furnace slag (GGBFS), supplied by Heidelberg Materials UK, from Ribblesdale and Port Talbot works, respectively were used as the main binders in this study. The word 'binder' in this study refers to the mix of CEM I, GGBFS (in this paper also referred to as 'slag') limestone powder and anhydrite. Limestone powder (conforms to BS 7979 [28]) supplied by LKAB minerals UK, and anhydrite supplied by Heidelberg Materials, UK were also used in this study. Anhydrite was added to maintain the total SO_3 content at 3 wt% for sulfate balance which influences the early-age reaction kinetics of the clinker phases and supplementary

Table 1
Oxide compositions and physical properties of CEM slag, limestone and anhydrite.

XRF oxide composition				
	CEM I	Slag	Limestone	Anhydrite
Al_2O_3	4.51	11.52	0.27	0.8
SiO_2	18.6	35.56	0.94	2.37
CaO	62.59	40.25	55.82	38.35
SO_3	5.72	2.41	0.09	52.18
K_2O	0.31	0.5	0.03	0.19
Na_2O	0.18	0.3	0.2	0.34
MgO	2.39	7.98	0.69	1.4
TiO_2	0.22	0.57	–	–
MnO	0.06	0.2	–	–
Fe_2O_3	2.08	0.31	0.06	0.25
Trace	0.39	0. 41	0.09	0.34
LOI[a]	2.95	–	41.8	3.8
Physical properties				
Particle size distribition d_{50} (μm)[b]	17.1	14.1	11.9	
Density (kg/m^3)[c]	3136	2917	2728	
BET specific surface (m^2/g)[d]	1.38	1.29	1.04	

[a] Loss on ignition (LOI) determined by wt. (%) change at room temperature and weight after 2hrs heating at 900 °C and ambient cooling.
[b] Determined with a Malvern Mastersizer 2000 laser diffractometer, using a dry dispersion unit.
[c] Measured using a helium pycnometry.
[d] Nitrogen adsorption-desorption measurements were conducted at 77 K using a Micromeritics Tristar 3000 to ascertain the Brunauer-Emmett-Teller (BET) surface area.

cementitious materials, as well as the later-age properties of the hydrated cements [29]. Table 1 shows the oxide compositions of the materials used in this study, determined by X-ray fluorescence (XRF) spectroscopy using a Rigaku ZSX Primus II, with the fused bead preparation method. The quality ($CaO + Al_2O_3 + MgO/TiO_2 + SiO_2$) and basicity ($CaO + MgO/Al_2O3 + SiO_2$) coefficients of the slag used are 1.65 and 1.02 respectively. The physical properties, including average particle size, density and BET surface area, are reported in Table 1.

The aggregates used for concrete production were crushed quartzite. The particle size distribution of sand, 10 mm and 20 mm aggregates used for concrete production are reported in Ref. [27]. The water absorption of sand, 10 mm and 20 mm aggregates was determined according to BS EN 1097–6:2022 (18), and the values for the different aggregate fractions were 1.9 (sand), 1.2 (10 mm aggregate) and 1.1 (20 mm aggregate) % respectively. Water corrections due to aggregates water absorption were factored in the concrete mix designs.

2.2. Concrete mix design and mixing

The mix design used for concrete production is reported in Table 2. The total binder content for all the concrete mixes was kept at 320.3 kg/m^3 to conform with the specification in the BS EN 206–2021 [30] recommended for carbonation induced corrosion (XC1-4) and chlorides XS (1–2) and XD(1–3) exposure classes. The ratio of water to binder was kept constant at 0.5 for all mixes. The cement used in this study, herein referred to as N, NS, NSL, N2L as shown in Table 2, for plain CEM I, CEM I replaced with 50 wt.% binary GGBFS, ternary GGBFS (40 wt. %)-limestone (10 wt.%) and ternary GGBFS (30 wt.%)-limestone (20 wt. %), respectively.

Cement constituent and dried aggregates were homogenised in a planetary mixer, initially for 5 min followed by the addition of water, and the mixture was further mixed for 5 min. The fresh properties of the concretes were determined, followed by casting specimens in plastic/metallic moulds as per BS EN 12390–2:2019 [31], and demoulded after 24 h. Demoulded specimens were stored in a curing room until testing. Fresh properties tested included slump, spread, air content and density following standardised procedures BS EN 12350–2:2019 [32], BS EN 12350–5:2019 [33], BS EN 12390–7:2019 [34] and BS EN 12350–6:2019 [35] respectively. The procedures are reported by the authors elsewhere [27]. All concrete mixes in this study were cured in a fog room (temperature 20 ± 3 °C and 95 % relative humidity (RH)) until testing.

2.3. Methods adopted for concrete testing

2.3.1. Carbonation depth evolution

The carbonation performance of concretes was investigated by monitoring their carbonation depths at various times of exposure. The exposure to accelerated carbonation was conducted according to the BS EN 12390–12:2020 [36]. For specimens intended for carbonation exposure, the cast concretes were wrapped with plastic film before demoulding after 1 day. After 28 days curing period, concrete prisms (75 × 75 × 200 mm) were air-dried and then sealed with self-adhesive aluminium foil at the ends and transferred for preconditioning at 20 °C, 57 ± 3 % relative humidity (RH) for 14 days. The pre-conditioned samples were then transferred to a climate-controlled chamber and exposed to accelerated 3 % [CO_2], 57 ± 3 % RH, and 20 °C. This exposure condition was adopted for the accelerated carbonation testing as per the recommendation of the standard EN 12390-12 [36], and also as a representative condition for determining the carbonation resistance of concrete via accelerated methods [37]. Carbonation depths were measured at exposure durations of 7, 28, 70 and 100 days. Simultaneously, concrete specimens were kept in an environmental chamber at the same RH and T without CO_2; thus, at environmental CO_2 conditions (350–400 ppm), and monitored for up to 365 days.

Carbonation depths were measured on freshly split surfaces at testing age and sprayed with 1 % phenolphthalein solution and measuring depth in regions changing from fuchsia to colourless. This indicator was prepared according to the standard BS EN 12390–12:2020 [36], using 100 % isopropanol instead of water as dissolving media, as it resulted in well delineated carbonation depths particularly in CEM I at early ages.

2.3.2. Transport properties studies post-carbonation

For studying the impact of carbonation on the transport properties of concretes, samples were systematically exposed to carbonation and then subjected to chloride or water ingress testing. In order to replicate cored cover concrete samples derived from existing concrete infrastructure for durability testing, cylindrical specimens were exposed to unidirectional carbonation as illustrated in the schematic diagram Fig. 1. 28 days cured Ø100 × 200 mm cylindrical samples were surface dried, coated on the circumference with Sika® primer MB (3A (resin):1B (hardener) [38]) and allowed to dry in a fume cupboard over 24-h. Post drying, they were cut into Ø100 × (50 ± 5) mm and one of the as-cut surfaces of the concrete was sealed with sufficient layers of self-adhesive aluminium, so that only one as-cut surface was available for CO_2 to ingress. These Ø100 × 55 mm samples were used for evaluating the chloride permeability, water absorption and for monitoring the carbonation depths after natural or accelerated carbonation exposure. It was ensured the carbonated surface was exposed to the NaCl solution in all cases. Similarly, for water ingress studies, the immersed surface was the carbonated surface.

2.3.2.1. Water absorption rate/sorptivity and porosity determination.

Capillary water absorption was conducted following the BS EN 13057:2002 [39] on two partially carbonated cylindrical specimens (coated on the circumference) with a thickness of 50 ± 5 mm after 28 and 100 days of exposure (preceded by 28 days of curing and 14 days of preconditioning). The mass changes were determined at predefined times up to 15 days. Prior to the test, samples were preconditioned by drying in a ventilated oven at (105 ± 5) °C, according to Ref. [40], until a constant mass was achieved in 7 days. This standardised preconditioning approach was adopted so the results can be compared with those obtained in real practice and not only used for research purposes. Post-oven drying; specimens were cooled to room temperature in a desiccator for 24 h until testing. After the sorptivity test, specimens were

Table 2
Concrete mix design (kg/m^3 of fresh mix).

Constituents	Mix ID			
	N	NS	NSL	NS2L
CEM I 52.5N	320.3	164.0	165.6	167.2
Slag	–	155.4	125.6	93.2
Limestone	–	–	28.3	59.0
Anhydrite	–	0.8	0.8	0.8
Water	160.2	160.2	160.2	160.2
Sand	651.8	648.8	648.2	647.5
10 mm Aggregates	237.7	236.6	236.4	236.1
20 mm Aggregates	950.8	946.5	945.5	944.5

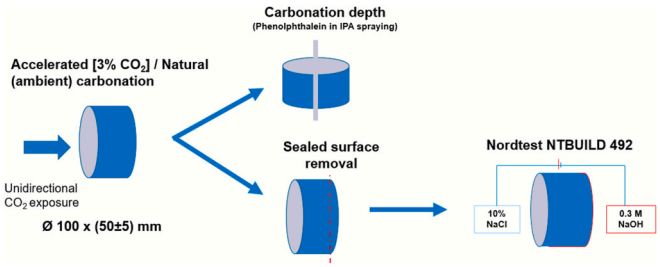

Fig. 1. Schematic diagram of experimental methodology for investigating effect of carbonation of transport properties of concrete.

vacuum saturated in water for 24 h, from which the porosity was calculated from the ratio of their weight (%) changes to the volume. The water absorption (mass%) was determined as the difference between dried and saturated mass expressed as a percentage.

2.3.3. Bulk conductivity

Bulk conductivity measurements of partially carbonated concretes were conducted on cylindrical samples (100Ø × 50 mm) intended for chloride permeability testing. This test was carried out according to the automated procedure described in the ASTM C 1760 [41], which entails the application of a potential difference of 60 V for 1 min, from which results can be recorded in mS/m in a Germann-supplied Proove'it software. Two cylindrical specimens per concrete mix were tested for each of the carbonation exposure conditions (natural or accelerated) at two exposure durations considered in the study.

2.3.3.1. Resistance to chloride permeability. The chloride permeability of the partially carbonated concretes was studied on two concrete specimens (100Ø × 50 mm) after 28 and 100 days of exposure in accordance with the Nordtest NTBUILD 492 chloride migration test [42]. Test pieces were preconditioned in lime solution under vacuum for 24 h followed by the chloride migration test using the Germann supplied instrument, PROOVE'it set up. Predetermined voltages were applied on samples centralised in compartments containing 10 wt.% NaCl solution and 0.3 M NaOH as catholyte and anolyte solution, respectively on either side. The carbonated surface was attached to the catholyte in all cases. Following a predefined test duration, tested samples were axially split, and their chloride penetration depth measured from white precipitates formed on samples by after spraying 0.1 M $AgNO_3$ on the freshly split surfaces. The average chloride depths (7 chloride depth measurements per halved cylinder), initial and final temperature, and the applied voltage were used as input for computing the D_{nssm} (non-steady-state migration coefficient, $\times 10^{-12}$ m^2/s) as per [42].

2.3.4. Post carbonation dimensional stability and compressive strength

2.3.4.1. Compressive strength. For all naturally or accelerated carbonated concretes, the residual strength was determined at different exposure durations. The compressive strength test was conducted for concrete at 6 kN/s loading rate in accordance with BS EN 12390–3:2019 [43] using a 3000 kN capacity MATEST crusher, using 75 mm side concrete cubes sawn from 100 days carbonated 75 × 75 × 200 mm prisms. The strength of partially carbonated concretes was determined on the specimen directly after the corresponding carbonation exposure without water saturation on the specimen.

2.3.4.2. Dimensional changes. Dimensional changes during accelerated carbonation were measured on 75 × 75 × 200 mm concrete prisms using 120Ω, 60 mm surface mounted linear strain gauges. These were attached to two lateral sides of the specimens. As the samples were exposed to accelerated carbonation inside a climatic chamber, proprietary battery-powered wireless data loggers, *V-link 200* supplied by *Microstrain* instruments were used. The data loggers were interfaced with the *SensorConnect* software for remote transmission, thus reducing interference with the carbonation experiment. Dimensional changes data were initially collected during the initial 14 days of pre-conditioning (57 ± 3 % RH, and 20 °C), as per the accelerated carbonation standard recommendation [44], and continued when the prisms were transferred to the climatic chamber and exposed to 3 % [CO_2] accelerated carbonation for further 28 days. A corresponding sample was kept under natural-carbonation, and dimensional changes data was collected in a climatic chamber without CO_2. The dimensional changes were measured in one specimen per concrete mix upon exposure to natural and accelerated carbonation. This due to the space restrictions inside the climatic chambers used, limiting the number of specimens that could be tested at a given time.

Acknowledging the several phenomena that are taking place simultaneously in the concrete, which influence the dimensional changes of tested specimens, including the carbonation reactions, continued cement hydration in the non-carbonated regions of the specimens, and the specimen's desiccation during the testing period, the results from these tests are not referred to as carbonation shrinkage, which is the shrinkage caused due to carbonation reactions alone. Nevertheless, the results provide novel insight into the influence of carbonation exposure conditions on the dimensional stability of the GGBFS-containing concretes.

2.4. Results and discussion

2.4.1. Carbonation depth evolution in binary and ternary slag-blended concrete

Fig. 2(a) and (b) shows the carbonation depth evolution under accelerated exposure conditions. The results reveal an increased rate of carbonation in the slag containing concretes with (NS) or without limestone (NSL, NS2L) relative to CEM I (N). The overall accelerated carbonation coefficients corresponding to the slope of a linear regression for each mix design are reported in Table 3. It can be seen that for the slag-containing mixes, NS, NSL and NS2L exhibited comparable carbonation coefficients when determined up to 100 days of accelerated carbonation.

The carbonation depth evolution of concrete mixes under natural exposure for a period of 365 days is shown in Fig. 3(a). The average carbonation coefficients tabulated in Table 4 showed increased depths in NS, NSL and NS2L relative to the CEM I at all exposure times, consistent with the observations under accelerated carbonation exposure (Fig. 2). However, for slag-containing concretes with (NSL and NS2L) and without limestone (NS), the values of the carbonation coefficients determined after exposure to accelerated conditions are twofold greater than those determined after natural carbonation exposure. These results are consistent with the findings reported by Proske et al. [19] who also identified a reduced carbonation resistance in composite concretes compared to CEM I, particularly when evaluated under accelerated carbonation conditions, but a negligible effect of limestone addition on the carbonation coefficient of composite concrete, compared with the binary ones. The reduced carbonation resistance of the composite cements concrete is attributable to their reduced portlandite content in the binder, consistent with a reduced clinker concrete, which reduces the CO_2 buffer capacity compared to CEM I systems [12].

Accelerated carbonation testing is conducted to infer the carbonation potential of concrete when exposed to natural environmental conditions. When concrete is exposed to similar environmental conditions (RH and T) with the CO_2 concentration as the only varying parameter, the natural and accelerated carbonation coefficients can be calculated according to Equation (1) [45], which is derived by Fick's law.

$$\frac{K_{Nc}}{K_{ACc}} = \frac{\sqrt{C_{NC}}}{\sqrt{C_{Acc}}} \quad \text{Eq. 1}$$

Where; K_{ACC} = Accelerated carbonation coefficient (mm*day$^{-0.5}$); K_{NC} = Natural carbonation coefficient (mm*day$^{-0.5}$); C_{ACC} = CO_2 concentration under accelerated carbonation (3 %); and C_{NC}(mm) = CO_2 concentration under natural carbonation (0.04 %)

The estimated K_{NC} considering the K_{ACC} values when applying this equation are reported in Table 5, where it is identified that the estimated carbonation coefficients (within error margins) are comparable to those determined experimentally. This demonstrates that for the experimental conditions adopted in this study, this correlation is suitable for predicting the natural carbonation coefficients of the CEM, and slag-blended concretes tested. However, such observation is limited to the testing conditions adopted in this study, where concretes were kept at similar RH and temperature upon natural or accelerated carbonation

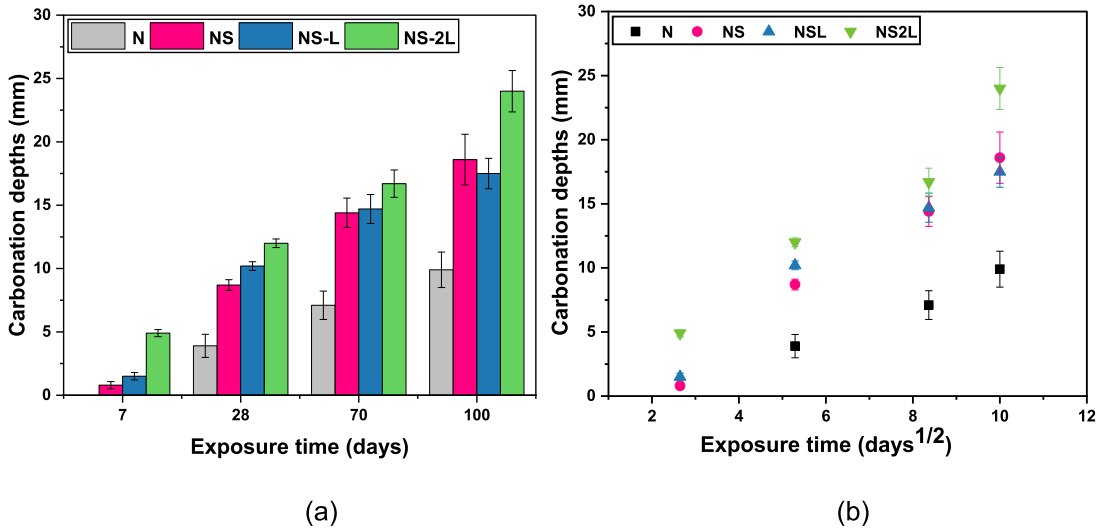

Fig. 2. (a) Carbonation depth of concretes exposed to accelerated carbonation up to 100 days and (b) the correlation between accelerated carbonation depth and the square root of time. The values reported correspond to the average of 16 readings (four per side), and error bars correspond to one standard deviation of such measurements.

Table 3
Accelerated carbonation coefficient (mm*days$^{-0.5}$) of concrete prisms based on the slope of the linear regressions of results in Fig. 2 (b).

Mix ID	N	NS	NSL	NS2L
Carbonation coefficient (mm*days$^{-0.5}$)	1.21 ± 0.16	2.65 ± 0.24	2.60 ± 0.45	2.45 ± 0.23
R^2	0.97	0.98	0.92	0.97

exposure to ensure comparable hydration and saturation degree of the specimens tested, to minimise the number of variables that might lead to different carbonation rates. It is worth noting that such a relation should not be adopted in the case that the RH and T of exposure under natural carbonation conditions (e.g. ambient unsheltered exposure), are completely different to that of the accelerated carbonation testing conditions [37]. Specific studies exposing concrete mix design to in-service environmental conditions are required to gain a good understanding of their natural carbonation performance.

2.4.1.1. Carbonation depth predictions and compliance with BS 8500-1. Fig. 4 shows a 100-year prediction of the carbonation front progression determined applying Equation (1), considering expose conditions adopted in this study, and expressed as:

$$K_{Nc} = K_{Acc} * \frac{\sqrt{C_{NC}}}{\sqrt{C_{Acc}}} = K_{Acc} * \frac{\sqrt{0.04}}{\sqrt{3}} = 0.115 = 0.1K_{Acc} \quad \text{Eq. 2}$$

Where; K_{ACC} = Accelerated carbonation coefficient (mm*day$^{-0.5}$); K_{NC}

Table 4
Natural carbonation coefficient (mm*days$^{-0.5}$) of concrete prisms based of the slope of the linear regression of the results in Fig. 3 (b).

Mix ID	N	NS	NSL	NS2L
Carbonation coefficient (mm*days$^{-0.5}$)	0.12 ± 0.02	0.21 ± 0.02	0.22 ± 0.01	0.26 ± 0.01
R^2	0.90	0.97	0.99	0.99

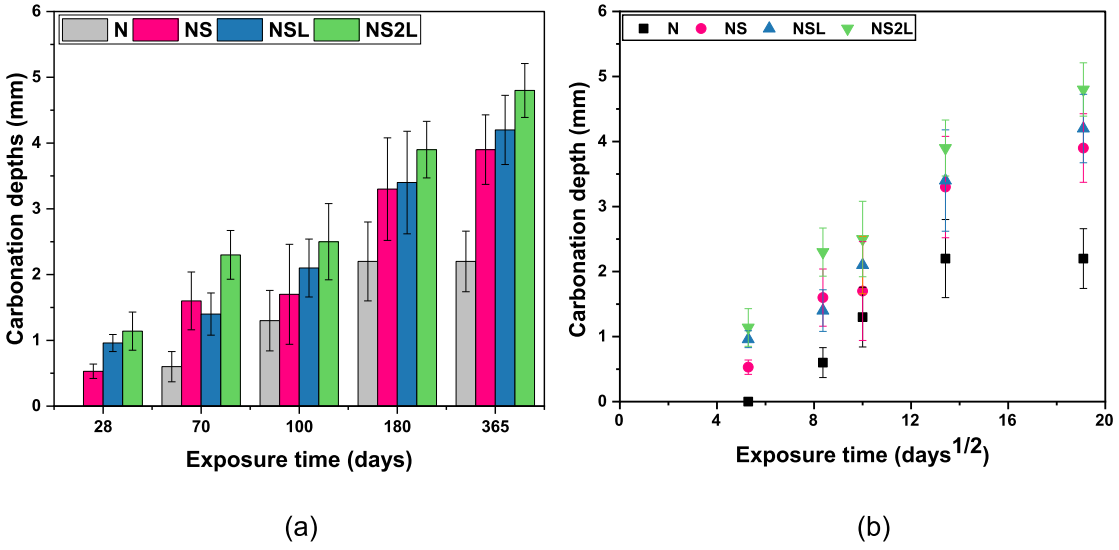

Fig. 3. (a) Carbonation depth of concretes exposed to natural carbonation up to 1 year; and (b) the correlation between natural carbonation depth and the square root of time. The values reported correspond to the average of 16 readings (four per side), and error bars correspond to one standard deviation of such measurements.

Table 5
Estimated natural carbonation coefficient from accelerated carbonation coefficient based on Equation 1.

Mix ID	Measured (Experimental): [a]K_{NC}	Measured (Experimental): [a]K_{ACC}	Estimated K_{NC} from K_{ACC} at 3 % [CO_2]
	Slope	Slope	
N	0.12 ± 0.02	1.21 ± 0.16	0.14 ± 0.01
NS	0.21 ± 0.02	2.65 ± 0.24	0.31 ± 0.02
NSL	0.22 ± 0.01	2.60 ± 0.45	0.30 ± 0.04
NS2L	0.26 ± 0.01	2.45 ± 0.23	0.28 ± 0.02

[a] K_{ACC} = Accelerated carbonation coefficient (mm*day$^{-0.5}$); K_{NC} = Natural carbonation coefficient (mm*day$^{-0.5}$).

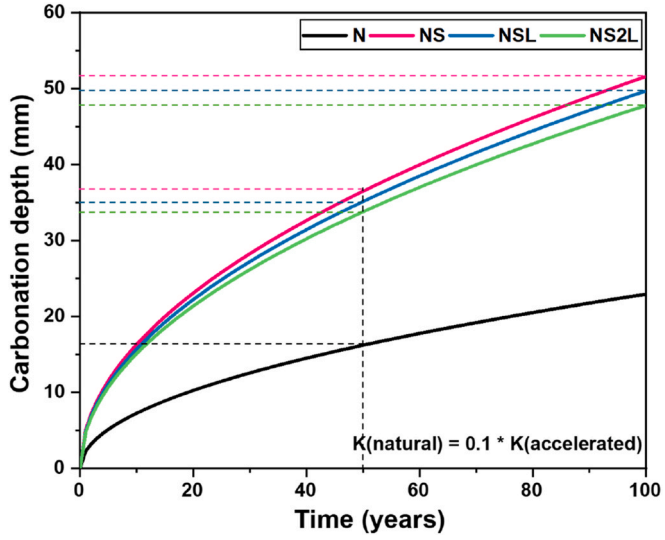

Fig. 4. 100-year carbonation depth prediction of the concrete mixes evaluated.

= Natural carbonation coefficient (mm*day$^{-0.5}$); C_{ACC} = CO_2 concentration under accelerated carbonation (3 %); and C_{NC}(mm) = CO_2 concentration under natural carbonation (0.04 %)

The CEM I concrete consistently exhibit a reduced carbonation depth up to 100 years of exposure relative to NS, NSL and NS2L, while all the slag-containing concretes with or without limestone will exhibit comparable depths, demonstrating that the partial substitution of slag by limestone is unlikely to have an effect on the long-term carbonation performance of the concretes evaluated. Correlating the predicted carbonation depth with the prescribed cover layer depths in accordance with standards, for example with BS-8500:1:2023 [22] which recommends a minimum concrete cover layer depth for carbonation exposure classes, enables identifying the practical relevance of the results reported here.

The cover layer depths predicted for the concretes evaluated here after 50 or 100 years of natural carbonation exposure are tabulated in Table 6. While high carbonation depths are evident in concretes made with slag-containing cement, the predicted carbonation depths are almost half of the minimum concrete cover value (~65 mm) for 50-year service life recommended by the BS 8500–1:2023 for concretes incorporating multicomponent cement systems (based on 28 days design strength, C25/30 in this study). Additionally, considering that carbonation results obtained when testing concrete under sheltered conditions often report higher depths than those obtained when the material is exposed to unsheltered conditions [46], it can be anticipated that concretes made with slag-limestone composite cement will perform satisfactorily in field conditions. However, caution needs to be exercised in these predictions by validation with long-term carbonation depth monitoring under environmental exposure conditions relevant to the in-service ambient condition to which the concrete is going to be exposed and the need to account for the effect of loading on the carbonation progress.

Table 6
Predicted natural carbonation depths at 50 and 100 years compared to the BS 8500–1:2023 recommended cover depth for concrete containing carbon reinforcing steel or prestressed elements for corrosion-induced carbonation (XC3: moderate humidity).

Concrete Mix ID	50 years Carbonation depth (mm)	50 years recommended Cover depth (mm)*	100 years Carbonation depth (mm)	100 years recommended cover depth (mm)**
N	16.2	45 + Δc	22.9	60 + Δc
NS	36.5	≥65 + Δc	51.6	No classification for C25/30
NSL	35.1		49.7	
NS2L	33.8		47.8	

Δc = allowance for workmanship; *values taken from Table A.4.A and ** Table A.5.A reported in the BS8500–1:2023 standard, respectively.

According to the BS8500–1:2023, a C25/30 concrete, independent of the composition of the binder, is unsuitable for structural applications for an exposure class XC3 (moderate humidity) at risk of corrosion induced by carbonation intended for 100 years' service, therefore a minimum concrete cover layer recommendation is not provided. However, considering the minimum cover depth specified for CEM I concrete in this standard, and the carbonation depth values predicted for the slag-containing concretes (Table 6) evaluated in this study, slightly higher cover depths than those recommended for CEM I concrete (60 mm) will be sufficient to ensure that the carbonation front does not reach the steel reinforcement.

2.4.2. *Compressive strength of carbonated concretes*

Fig. 5 (a) shows the compressive strength evolution of carbonated concrete after 100 days of natural or accelerated carbonation, along with the tested compressive strength after 365 days of natural carbonation exposure. It is identified that the compressive strength of concrete made with composite cements are comparable to those of CEM I concrete after 100 days of natural carbonation. The CEM I concrete (N) exhibited a significant increase in compressive strength at 365 days of exposure. The slag containing concrete (NS) exhibited a higher compressive strength gain than those with limestone addition (NSL and NS2L), whose strength gain is lower at higher quantities of limestone addition. Comparing the compressive strength evolution between 100 and 365 days in naturally carbonated samples, herein referred to as air curing (60 % RH), the compressive strength of partially carbonated samples are lower than those obtained in similar concretes mixes after 90 days and 365 days of moist curing as reported in Ref. [27]. This is conversely to what was reported by Atiş et al. [47] for slag-based concretes, who identified comparable compressive strengths independent of the curing type. An explanation for this discrepancy can be attributed to significant variations in the fineness of slag used in both studies, where slags with 3-folds less Blaine fineness were used in the current study. High fineness slag increases water demand. Thus, less evaporation water is expected in hardened concrete for the same water-to-binder ratio, which, when rapidly lost under air curing, would negatively impact the progress of secondary hydration. Additionally, high autogenous shrinkage in slag concretes [48,49], can potentially induce microcracking due to rapid loss of expected less amount of the evaporable water when using high Blaine slags. These combined effects negatively affect compressive strength development.

The residual strengths calculated as the ratio of the 100 days accelerated carbonated strength divided by the 100 days natural carbonated strength expressed as a percentage are shown in Fig. 5(b). N, NS, and NSL exhibited a comparable increase (~20 %) in the residual compressive strength when exposed to accelerated carbonation conditions, while the concrete with the higher limestone content (20 wt%) NS2L shows a 10 % reduction in the strength upon accelerated

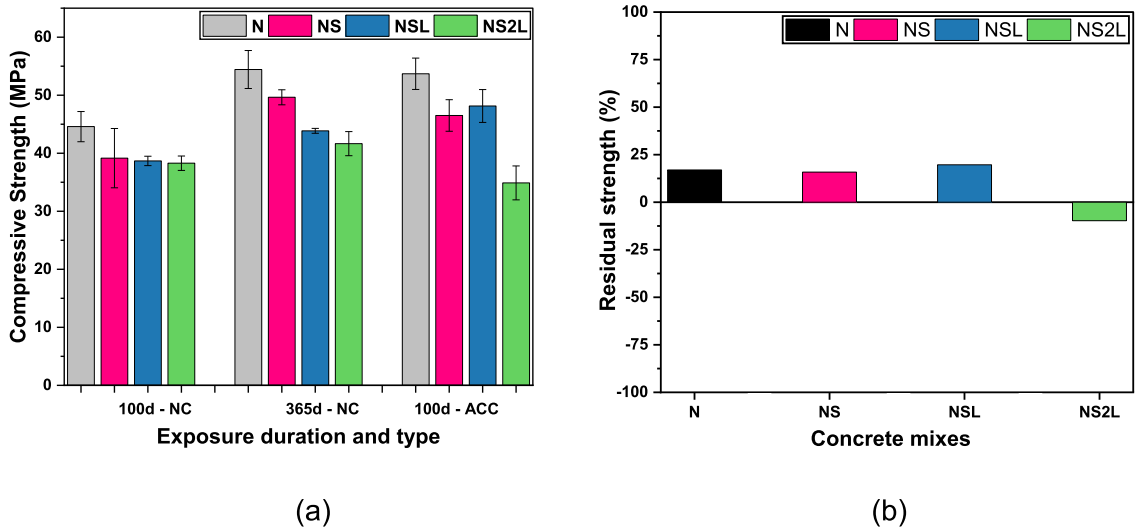

Fig. 5. (a) Compressive strength of concrete after 100 days of natural carbonation (NC), 365 days natural or 100 days of accelerated (ACC) carbonation; (b) Residual compressive strength (carbonated (ACC) strength/carbonated (NC) strength) after 100 days of exposure. Error bars correspond to the standard deviation of two measurements.

carbonation. This suggests that there is a limited content of limestone that can be added to these mixes without influencing the compressive strength when the material undergoes carbonation. It is worth noting that the compressive strength values of the 100-day accelerated carbonated NS2L concrete is 15 % greater than the 28-day design strength (30 MPa). This suggests that at long carbonation exposure durations, the continuous hydration of the slag containing cementitious binder compensates the microstructural changes induced by carbonation exposure so that the material exhibits compressive strength gains. The results also suggest that using the 28-day design compressive strength as a limiting factor for conformance to cover depths for XC3/XC4 exposure classes, excludes slag blended concrete mixes such as the ones evaluated in this study, which can be suitable for applications when 100 years' service life is required.

2.4.3. *Dimensional changes of carbonated concretes*

In practice, concrete would often undergo drying in combination with carbonation at moderate to low humidity conditions, and the dimensional changes of concrete structures that occur with the influence of load is referred to as shrinkage strain [50]. Fig. 6 (a and b) shows the shrinkage evolution of concrete mixes under natural carbonation or accelerated carbonation conditions. Under natural carbonation, the ternary blends (NSL and NS2L) show reduced shrinkage strain relative to binary slag (NS) and CEM I (N) concretes; binary slag (50 wt%) exhibits comparable shrinkage to CEM I under natural carbonation exposure. Meanwhile, under accelerated conditions slag containing concretes with (NSL and NS2L) or without limestone (NS) show reduced shrinkage relative to CEM I. However, the ternary blends (NSL and NS2L) similarly show reduced shrinkage to the binary slag concrete under accelerated conditions.

The difference between the strain measured in accelerated carbonated specimens, and the strain measured in specimens subjected to natural carbonation can be inferred as the shrinkage induced by accelerated carbonation, as the RH and T were kept constant during the

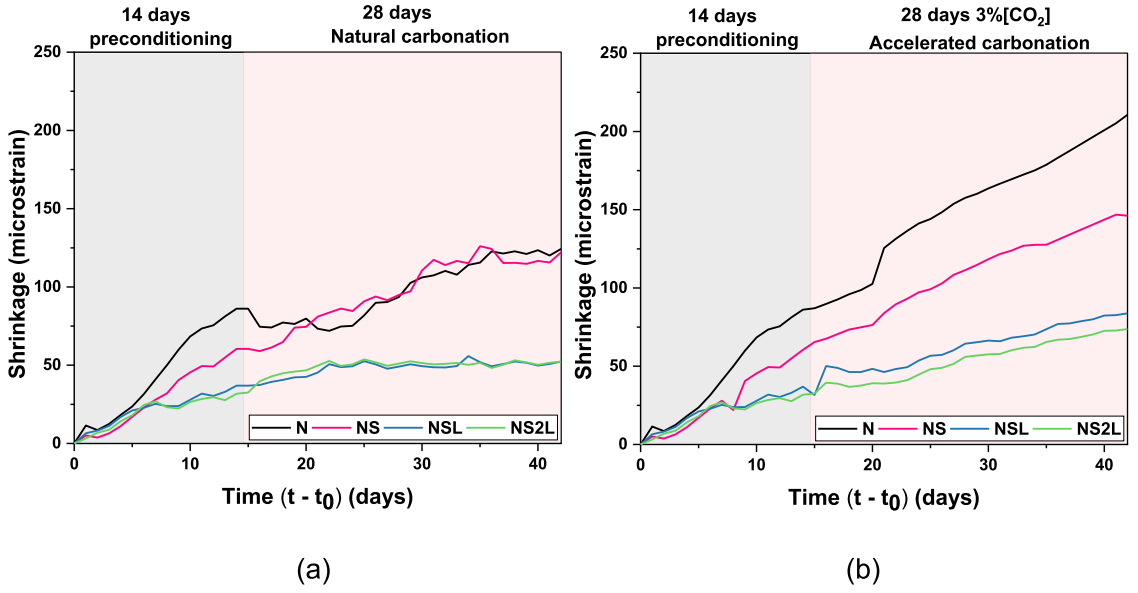

Fig. 6. Dimensional change evolution of CEM I, binary and ternary slag blended concrete mixes exposed to (a) natural (ambient) carbonation for 42 days or (b) 3 % [CO_2] accelerated carbonation for 28 days.

carbonation testing at both CO_2 concentrations, meaning that the desiccation and drying effects of the specimens during the testing duration are comparable. However, it must also be recognised that the extent of carbonation determines coarseness of the pore structure on the one hand, and the volume of water released from the carbonated phases. These may equally modify the resulting dimensional changes, but they cannot be separated at the macrosale, therefore, the aggregated impact is reported herein.

Comparable shrinkage values were observed during the specimens preconditioning for the two experiments (Fig. 6). However, significant differences in the shrinkage can be identified once the specimens were exposed to natural or accelerated carbonation. The specimens exposed to accelerated carbonation (Fig. 6 (b)) show increased shrinkage relative to natural carbonation exposure beyond the preconditioning period, for a similar exposure duration. Nonetheless, the increase in shrinkage due to carbonation is marginal in the ternary blends (NSL and NS2L) compared with the slag concrete without limestone which exhibits a higher shrinkage strain after 28 days of accelerated carbonation compared with the values observed in samples exposed to natural carbonation for a similar period. These observations are consistent with other studies [19,51] that have shown improvement in drying shrinkage of slag-limestone concrete relative to CEM I when assessed via experimental and analytical methods.

A plausible explanation of the performance identified under natural carbonation is linked to the microstructure differences of the cements evaluated. In blended slag systems, a reduced amount of hydration products form compared to CEM I at early curing durations [5], which translates into a reduced bound water removal during desiccation, in addition to restraining effects imposed by unreacted limestone acting as an additional filler particle similar to aggregates [52]. This is consistent with the fact that concretes with higher limestone addition (and consequently less slag) exhibited a reduced shrinkage, this being more noticeable as limestone addition increased (e.g. NS2L). The marginal increase in shrinkage under accelerated conditions suggests that increased carbonation rates in ternary mixes could potentially have a moderate impact on their dimensional stability in the long term.

As identified in Section 2.4.1, a composite cement exhibits a higher carbonation rate than binary and CEM I concrete, this being more noticeable under accelerated carbonation conditions. Liu et al. [53] identified in slag blended concrete that carbonation led to a coarser porosity, although a higher CO_2 concentration of exposure decreased the porosity of the carbonated sample independently of the slag content in the mix. This was attributed to the higher rate of C-S-H carbonation at higher CO_2 concentrations, releasing water to the system and potentially aiding clinker hydration as carbonation progresses. The water released during accelerated carbonation can also counteract the ongoing desiccation of the specimens upon testing, therefore limiting the extent of drying shrinkage experienced by the evaluated specimens. Since the difference in shrinkage strains was found to be negligible for composite slag concrete, independent of the limestone addition under natural or accelerated carbonation conditions. It is hypothesised that unreacted limestone particles in the materials are likely acting as filler particles limiting materials tendency for shrinkage from carbonation of reaction products. The results are consistent with the observed residual strengths in this study (Fig. 5 (b)), where increased carbonation shrinkage could have resulted in significant strength loss due to microcracking, which was not the case from the results reported in the study.

2.4.4. Studies on partially carbonated concrete cylinders

2.4.4.1. Carbonation depth evolution of carbonated cylinders. The carbonation depths of cylinders subjected to unidirectional carbonation are shown in Fig. 7(a) and (b) after natural and accelerated carbonation respectively. In all the exposure conditions assessed, NS, NSL and NS2L presented higher carbonation depth relative to CEM I, consistent with the trends exhibited by the carbonated prisms of similar concrete mixes (Fig. 3). As can be seen in Fig. 7(c), it is identified that the carbonation coefficients of prismatic specimens are comparable to those of cylinder specimens exposed to 1-dimensional CO_2 ingress.

The results in Fig. 8(c) demonstrate that similar carbonation depths are recorded for specimens of different geometries under the same carbonation exposure conditions such as those specified in the BS EN 12390–12:2022 [36].

2.4.4.2. Variation in water absorption properties in carbonated concretes. The water absorption characteristics of concrete give insight into the porosity and their pore structure connectivity. Thus, the admissibility of water into capillary pores serves as a useful durability indicator [54,55], and it is typically quantified by measurements such as the sorptivity coefficient and slope of the first linear section of the sorptivity profile (time t = 0 to saturation point). Sorptivity profiles of partially carbonated cylinders post 28 and 100 days of natural or accelerated carbonation exposure are shown in Fig. 8 (a–d). The sorptivity profiles show comparable trends, however, the difference in sorption properties can be seen in the concrete mixes quantified in Tables 7 and 8 as sorptivity coefficient and total water absorption respectively.

CEM I shows a decreased sorptivity coefficient after prolonged carbonation relative to 28 days carbonation, and independent of the carbonation exposure type. Meanwhile, the composite binders generally demonstrated increased sorptivity coefficient (all mixes, including NSL when considered with error margins) post 100 days carbonation irrespective of exposure type. That notwithstanding, comparing the mixes by specific exposure types and age, it is not conclusive that CEM I demonstrated reduced sorptivity coefficients relative to composite cements. For example, even though post 100 days of natural carbonation, NS, NSL and NS2L generally show an increase relative to CEM I, the 100 days post-accelerated carbonation (considered as the extreme scenario similar to longer-term natural carbonation) show comparable values for all mixes (including NSL when considered within error margins).

Findings in partially carbonated concretes exposed to natural conditions can be explained by the continuous hydration in the uncarbonated region (internal curing) relative to the carbonated section identified in the concretes evaluated. In the natural carbonated section of the specimens after 28 and 100 days of exposure, it is expected that the pore refinement characteristic of blended slag concrete counteract changes in porosity associated with decalcification of hydrated phases at slow carbonation rates, which potentially contributed to the overall lower initial water absorption coefficients relative to CEM I [56].

While CEM I coefficients reduce after 100 days of natural carbonation and composite cements increase, the changes are less detrimental (<8 %). The evident reduction in sorptivity coefficients of CEM I post 100 days of accelerated carbonation relative to 28 days, unlike when compared to NS, NSL and NS2L is attributable to the densification of microstructure due to carbonated phases in the pore system [57], and continued clinker hydration during the duration of the test. However, the comparable sorptivity coefficients under the severest conditions (post 100 days accelerated exposure) suggest that factors beyond carbonation-induced decalcification, influence the sorptivity under accelerated carbonation. It is also worth noting that the potential impact of carbonation shrinkage-induced microcracking is not prevalent considering the results reported in Section 2.4.3.

Table 8 shows the total water absorption of the concrete mixes. Under natural carbonation NS2L shows slightly higher water absorption at 28 days but exhibits comparable values by 100 days of ambient exposure to those of CEM I at 100 days, indicating that prolonged carbonation exposure is not inducing significant changes in water permeability. Similarly, for accelerated exposure conditions, despite composite concretes exhibiting an increased carbonation depth (Fig. 8) compared to CEM I, this did not translate into increased water absorption by 100 days of exposure.

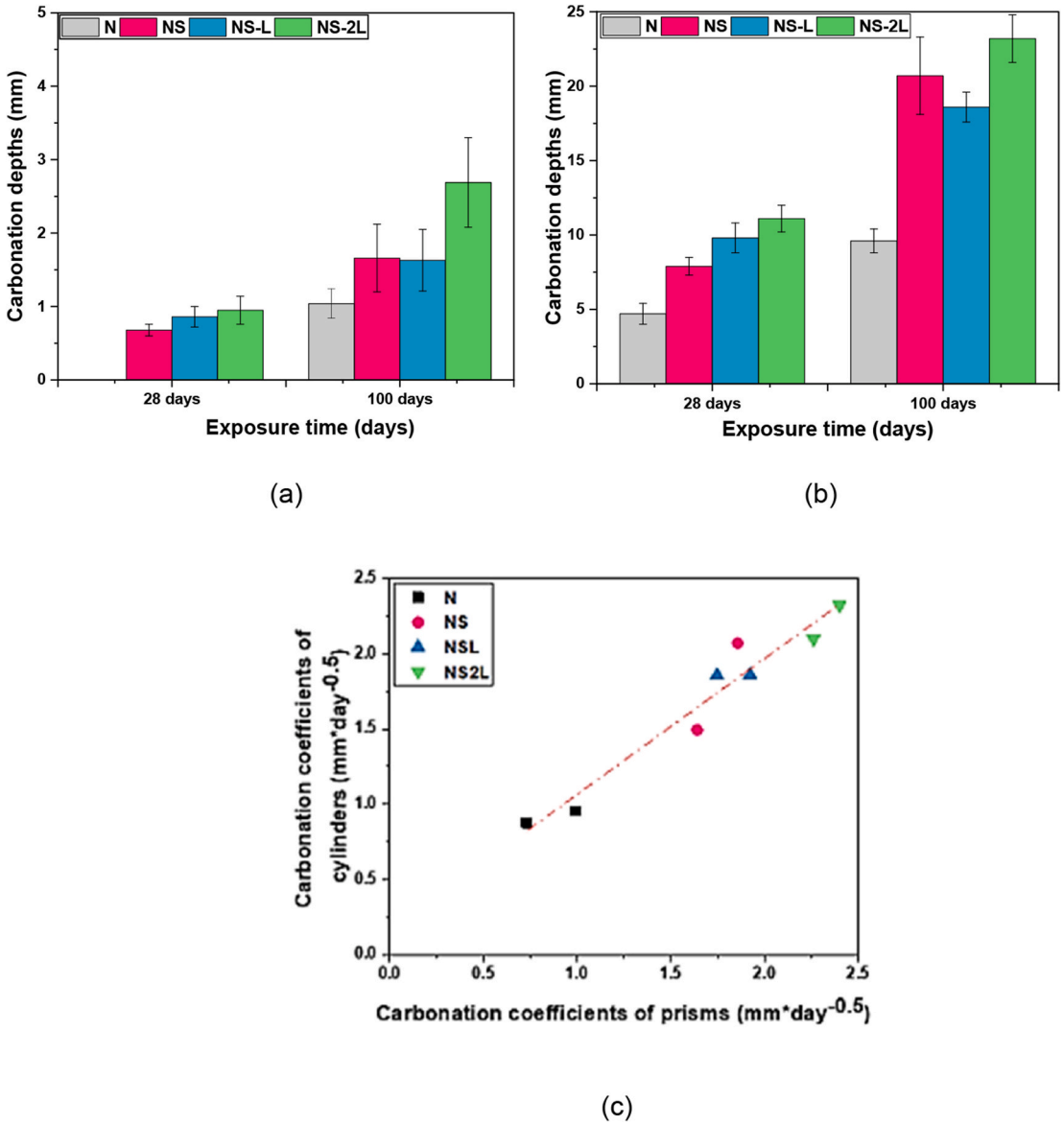

Fig. 7. Carbonation depth of concrete cylinders after 28 days and 100 days (a) natural, (b) accelerated carbonation exposure; and (c) correlation between accelerated carbonation coefficients (28 and 100 days) of prismatic and cylindrical specimens.

When the combined influence of carbonated (pore structure changes) and uncarbonated regions (continuous hydration and consequent pore refinement) on sorptivity are considered, it can be concluded that the addition of limestone does not have a significant impact on the water absorption properties of the ternary mixes. This is consistent with findings reported by Chen et al. [58], who demonstrated that limestone fines reduced water permeability and sorptivity in cured concrete. Thus, the uncarbonated region most likely undergoing hydration (albeit slow due to lower RH) could ensure resistance to moisture ingress due to ongoing pore structure refinement, which has a bearing on the overall moisture penetrability.

2.4.4.3. Changes in volume of permeable voids. The results of vacuum saturated porosity of the partially carbonated concrete mixes are shown in Fig. 9. There is no marked changes in porosity at the early and advanced carbonation exposure durations, irrespective of the exposure condition (natural or accelerated).

No significant changes in the total porosity are observed, consistent with the post-carbonation residual strength values (Fig. 5) of the evaluated concretes. Similarly, the potential influence of carbonation-induced pore structural changes appears less evident when considering the influence of both carbonated and uncarbonated regions. Considering the performance-based durability indicator of cementitious systems proposed by Baroghel-Bouny [59], the porosity values recorded for all the carbonated concretes evaluated correspond to medium to high durability performance, irrespective of the CO_2 exposure concentration or its duration.

2.4.4.4. Effect of carbonation on bulk conductivity. Fig. 10 (a–d) shows the bulk conductivities of concrete mixes after 28 days and 100 days of natural or accelerated carbonation exposure, superimposing the corresponding carbonation depths. The bulk conductivities of slag containing concretes with (NSL and NS2L) or without limestone (NS) are lower relative to CEM I (N), irrespective of the carbonation exposure type at 28 and 100 days. Under natural carbonation, the bulk conductivities of all concrete mixes are comparable for exposure durations of 28 and 100 days. Meanwhile under accelerated carbonation exposure, the bulk conductivity of CEM I is lower compared to corresponding natural carbonation values. Negligible changes are observed for NS, NSL and NS2L independent of exposure type or duration. The results suggest that

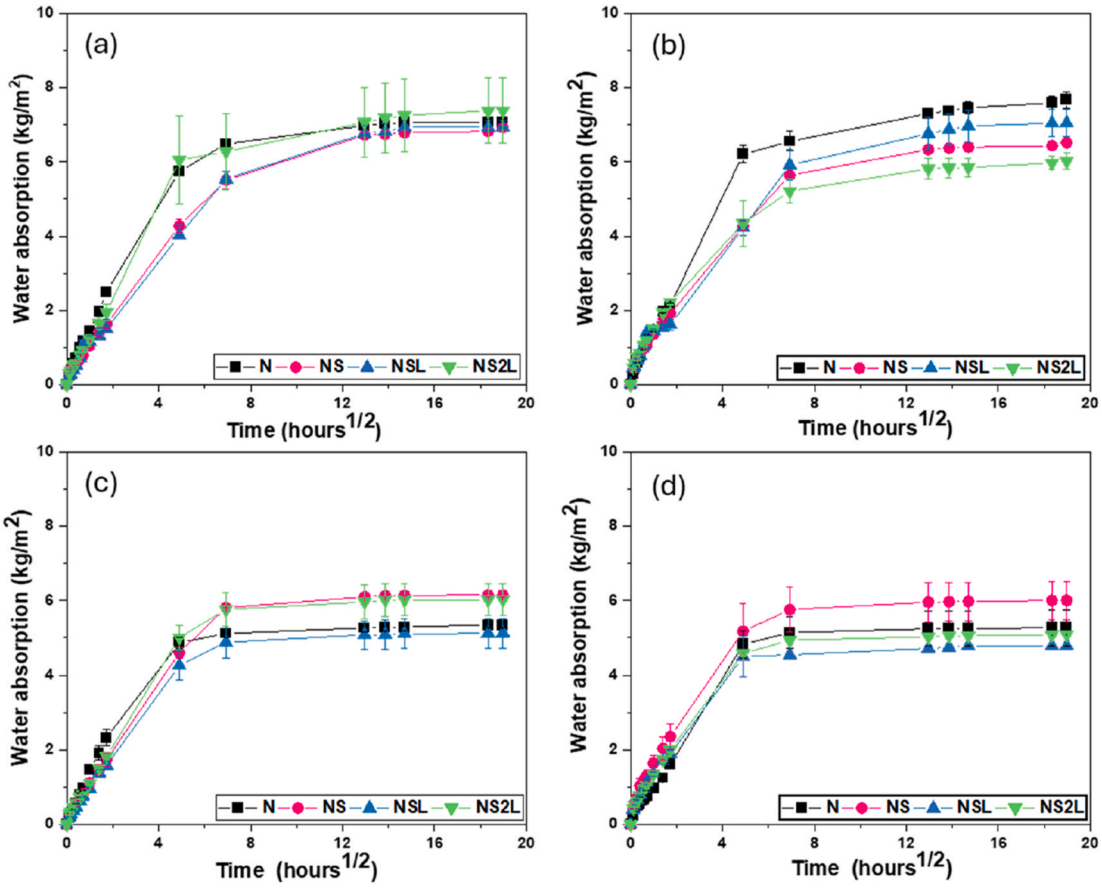

Fig. 8. Sorptivity profiles of CEM I, binary and ternary slag concrete mixes after 28 days of (a) natural or (b) accelerated; and 100 days of (c) natural or (d) accelerated carbonation exposure.

Table 7
Sorptivity coefficients (kg*m^{-2}*h$^{-0.5}$) of 28 days carbonated concrete mixes after natural or accelerated carbonation exposure. Error bars correspond to one standard deviation of two curves.

Mix ID	Natural carbonation		Accelerated carbonation	
	28 days	100 days	28 days	100 days
N	0.96 ± 0.12	0.79 ± 0.03	1.11 ± 0.06	0.94 ± 0.12
NS	0.79 ± 0.04	0.84 ± 0.001	0.77 ± 0.02	0.99 ± 0.21
NSL	0.78 ± 0.04	0.85 ± 0.12	0.79 ± 0.08	0.73 ± 0.30
NS2L	0.97 ± 0.25	0.99 ± 0.09	0.72 ± 0.11	0.90 ± 0.003

Table 8
Water absorption (%mass) of concrete mixes after 28 and 100 days carbonated of natural or accelerated exposure. Error values correspond to one standard deviation of two measurements.

Mix ID	Natural carbonation		Accelerated carbonation	
	28 days	100 days	28 days	100 days
N	5.38 ± 0.44	5.0 ± 0.32	5.8 ± 0.52	5.43 ± 0.14
NS	5.15 ± 0.10	5.66 ± 0.25	4.82 ± 0.24	5.44 ± 0.95
NSL	4.77 ± 0.14	4.91 ± 0.23	5.29 ± 0.24	4.48 ± 0.10
NS2L	5.51 ± 0.55	5.15 ± 0.20	5.27 ± 0.10	4.84 ± 0.08

the higher carbonation depth in NS, NSL and NS2L relative to CEM I does not translate into noticeable changes in bulk conductivity in all cases.

The results show a reduced bulk conductivity of CEM I concrete post accelerated carbonation, being more significant at the increased carbonation depth recorded. As can be seen in Fig. 10(d), the bulk conductivity at 100 days of accelerated carbonation reduces the bulk conductivity of CEM I to values comparable to those recorded in NS, NSL, and NS2L concretes. The reduction in bulk conductivity in CEM I with increasing carbonation depth is likely due to the calcite precipitation in the pore structure leading to densified microstructure [57].

The reduction in bulk conductivities with carbonation exposure doesn't apply to NS, NSL and NS2L, as the bulk conductivities were comparable independent of the exposure type and duration. The unnoticeable variation in bulk conductivity with increased carbonation depth in NS, NSL and NS2L suggests that other factors in addition to pore structural changes, including chemical factors such as ionic pore solution [60] may influence the performance, which is unaccounted for by the bulk conductivity measurements. However, the bulk conductivity results are somehow consistent with total porosity (Fig. 9) and water absorption properties (Table 7, Table 8) observed in the concretes after accelerated 100 days of carbonation exposures, where negligible differences were observed, even though higher carbonation depths were recorded. Moreover, no correlation exists between the bulk conductivity and porosities data in carbonated concrete as shown Fig. 11.

2.4.4.5. Impact of carbonation on chloride ingress. Fig. 12(a–d) shows the chloride permeability of the carbonated concretes, where it can be seen that CEM I concrete exhibits inferior chloride permeability compared to NS, NSL and NS2L for carbonation exposure conditions and durations assessed. While the chloride migration coefficient of all concrete mixes after 28 days and 100 days of natural carbonation are comparable, they increased upon accelerated carbonation. The increase in migration coefficients post-accelerated carbonation is more evident after 100 days of exposure, where higher values were observed in the concretes made with ternary cements (NSL and NS2L). It is worth noting, however, that, while the carbonation depth of NS2L concrete was

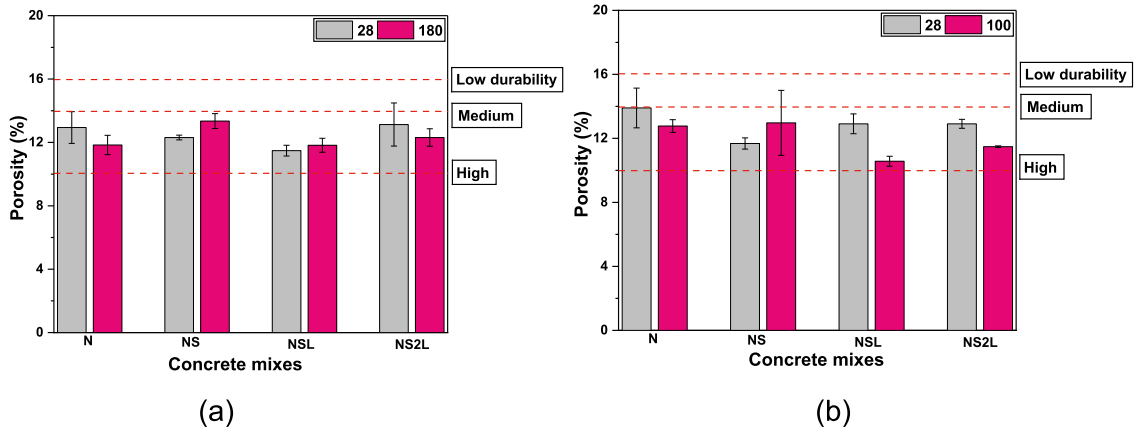

Fig. 9. Total porosity of carbonated of concrete mixes after (a) 28 and 100 days of natural carbonation; and (b) 28 and 100 days of accelerated carbonation exposure.

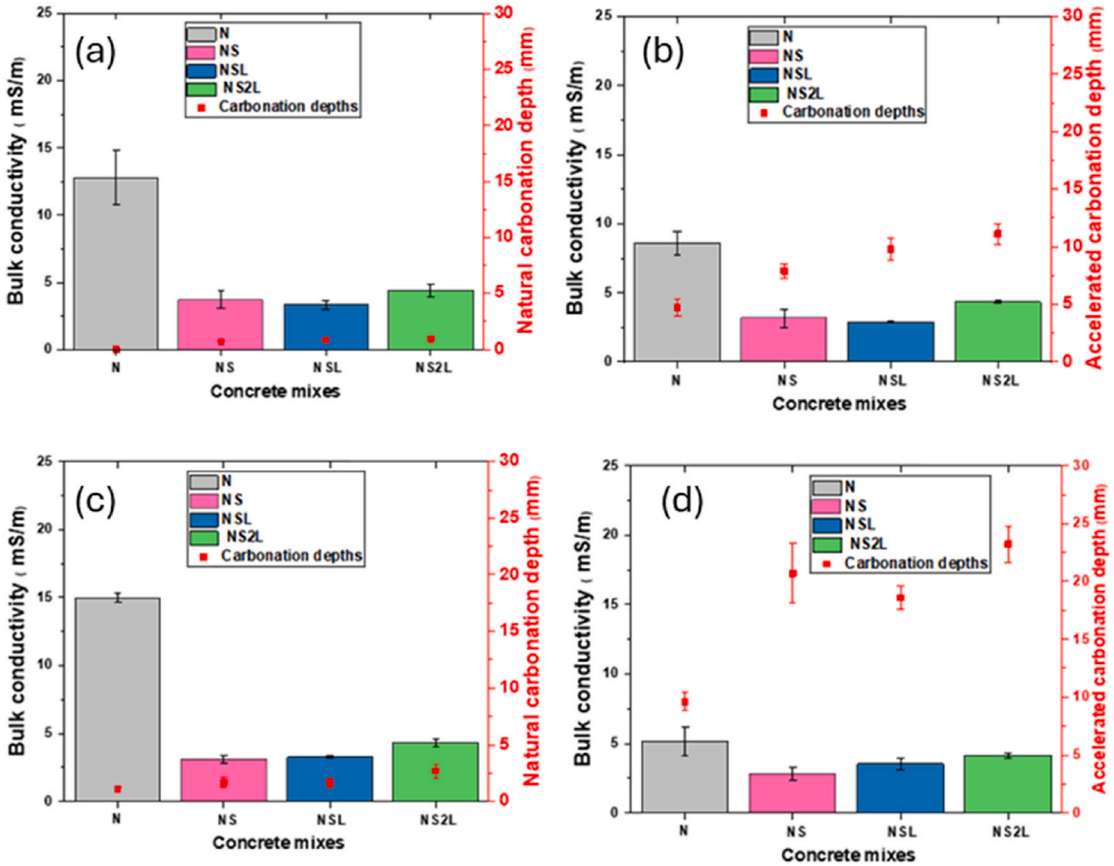

Fig. 10. Bulk conductivity (mS/m) of concrete mixes after (a) 28 days of natural carbonation (b) 28 days of accelerated carbonation, (c) 100 days of natural carbonation, and (d) 100 days of accelerated carbonation.

~three folds greater than in CEM I, the increased value in its chloride permeability is nearly still less than 50 % that of CEM I.

The results can be explained by a combination of physical and chemical factors. Slag addition to NS, NSL and NS2L results in hydrates that can chemically bind/adsorb chlorides including aluminium-substituted calcium silicate hydrates (C-A-S-H), Mg-Al layered double hydroxide like phases, AFm phases and potentially AFm-CO_3^{2-} phases [61–63]. This favours a lower chloride migration in slag blended systems, with or without limestone addition, when compared to CEM I in all cases. However, the increase in chloride permeability with increasing carbonation depth in the composite cements (NSL and NS2L) can destabilise the chloro-complexes formed due to their sensitivity to reduced pH in the carbonated zone [64]. The physical factors influencing chloride permeability are linked to the refined pore structure, due to continuous hydration in the uncarbonated zone (albeit at a reduced rate), and pore volume changes in the carbonated zones. Such changes are expected to be more detrimental in NS, NSL and NS2L relative to CEM I due to their overall reduced carbonation depths (Fig. 2). However, at advanced accelerated carbonation durations, the chloride permeabilities of concretes made with blended cements are still significantly lower than those of CEM I. No correlation between the porosity (Fig. 14) and chloride permeability (Fig. 13) was identified in the concretes evaluated, as a wide range of chloride migration coefficients are reported to a given porosity value. This confirms that the

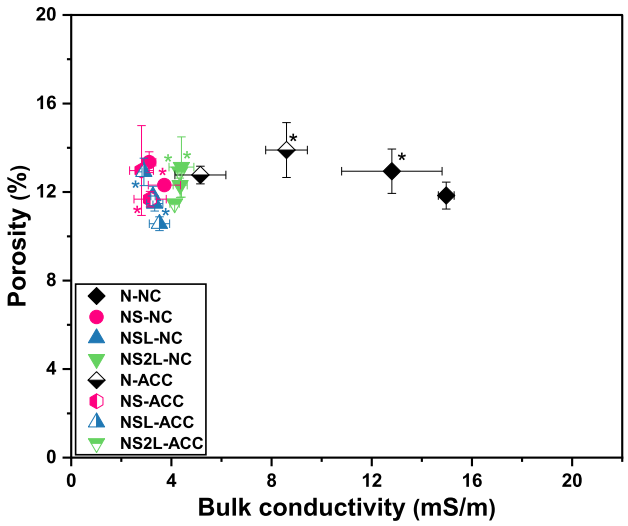

Fig. 11. Porosity Vs Bulk conductivity of concrete mixes after 28 and 100 days natural/accelerated carbonation. Note: Data points with or without asterisks (*) correspond to 28 or 100 days respectively].

chemical factors dominate the performance of slag-containing concretes when exposed to chlorides. While previous studies have shown significant changes in pore structure and electrical resistance in slag-limestone ternary binder [17], as no direct correlation between bulk electrical resistivity and porosity was identified in this study (Fig. 11), it is not possible to identify a correlation between the chloride migration coefficient and the bulk electrical resistivity, independently of the concrete mix or carbonation exposure condition. This further demonstrates the limitations of using bulk resistivity measurements to infer the durability performance of composite concrete in realistic condition where concrete may be carbonated.

The findings on the influence of carbonation on chloride permeability are consistent with other studies on binary slag [25], and ternary slag-fly ash [26] hardened mortars and concretes, which are largely

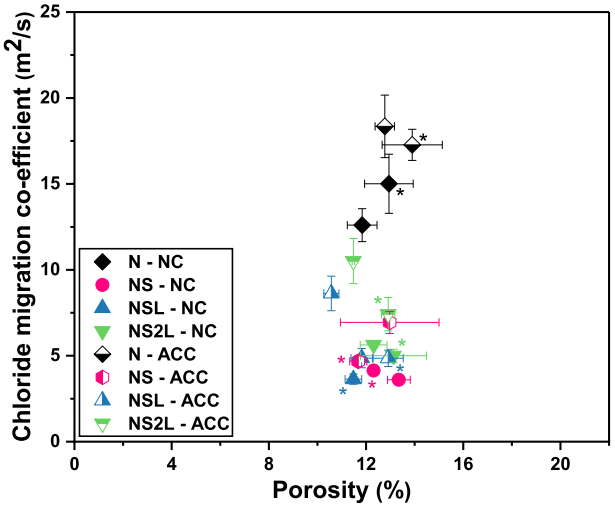

Fig. 13. Chloride permeability Vs porosity of concrete mixes after 28 and 100 days natural/accelerated carbonation. Note: Data points with or without asterisks (*) correspond to 28 or 100 days respectively].

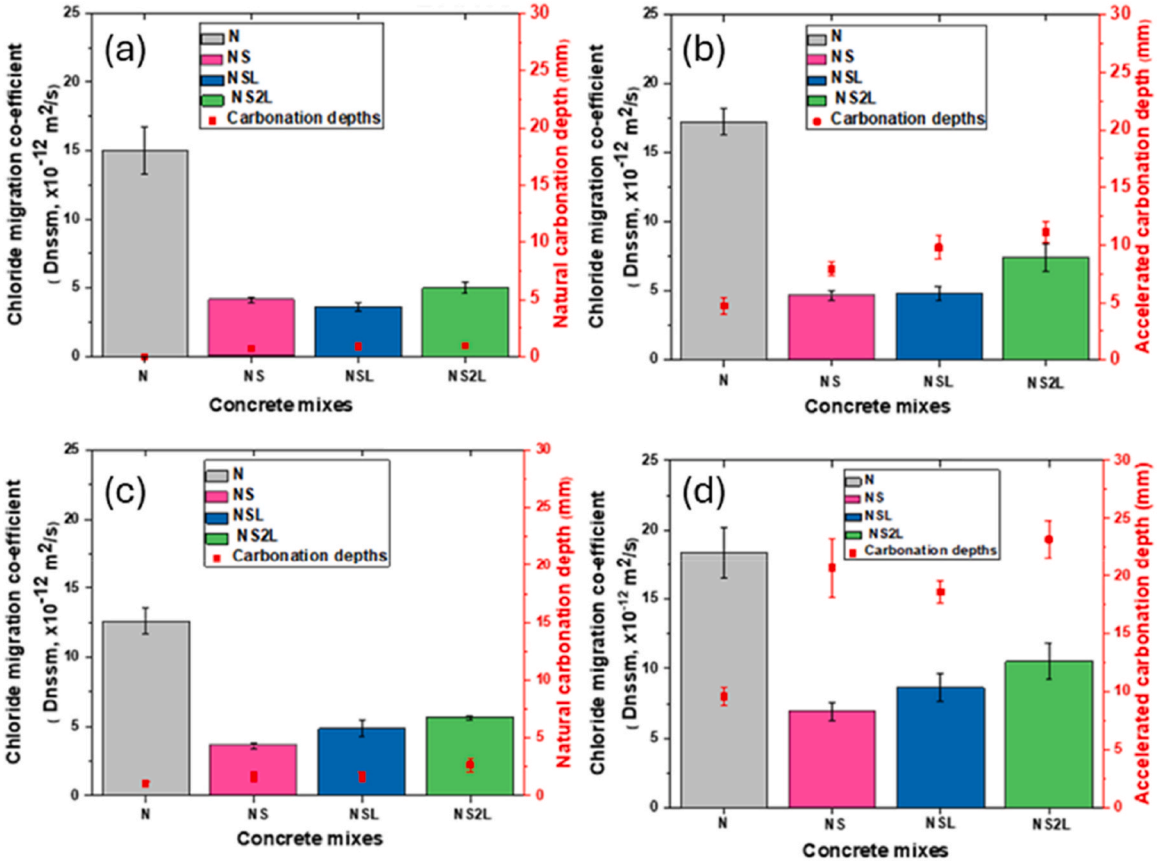

Fig. 12. Chloride migration coefficient (m^2/s) of concrete mixes after 28 days of (a) natural or (b) accelerated carbonation; and after 100 days of (c) natural or (d) accelerated carbonation exposure.

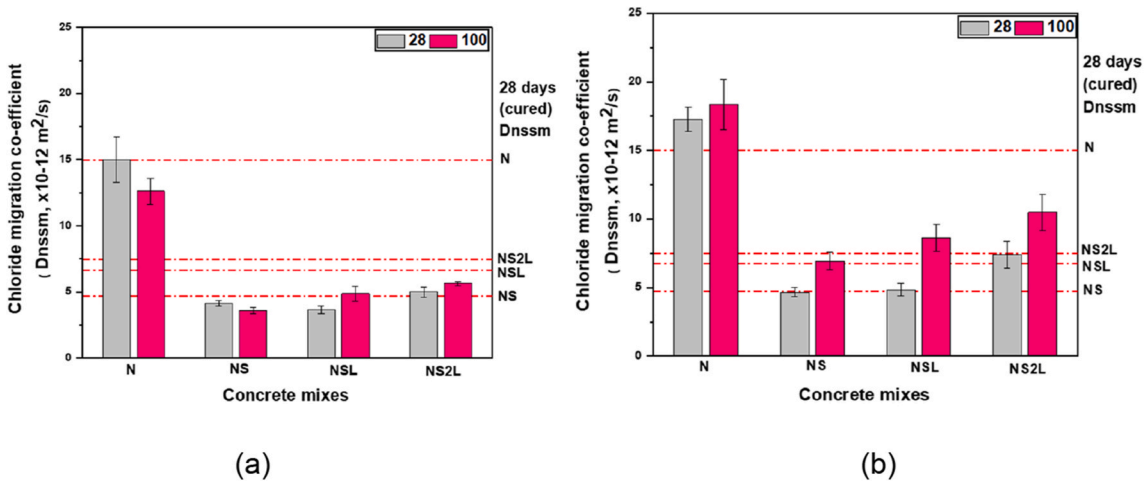

Fig. 14. Chloride permeability of concrete mixes after 28- and 100-days exposure to (a) natural carbonation or (b) accelerated carbonation. Dashed lines correspond to the coefficients determined in 28 day cured non-carbonated concrete reported in [27].

based on prolonged exposure to chlorides based on diffusion.

2.4.4.6. Impact of carbonation on chloride ingress relative to cured concrete. Towards assessing the extent of variations in chloride permeability due to carbonation, the post-carbonated chloride permeability values recorded in this study were compared to corresponding 28 days cured concretes (results reported in Ref. [27]) as shown in Fig. 14. In a previous study by the authors [27] using similar concrete mixes to those studied here, it was observed that chloride permeability reduced at extended curing durations (28–180 days), independent of mix design. This suggests the chloride migration coefficient of 28 days of cured concrete is much higher than what can be expected in a concrete structure designed for decades of service life. Thus, it can be argued that the worst performance of concretes post-carbonation can be assessed when benchmarked or compared to the 28-day cured performance indicator i.e. chloride migration coefficient here.

In Fig. 14 (a), it can be seen that all concrete mixes exposed to natural carbonation do not show any reduction in performance by 100 days of exposure, when compared to 28 days uncarbonated cured concrete. In Fig. 14 (b), it is identified that while CEM I exhibits an increased chloride migration coefficient post 28- and 100-days of accelerated carbonation, relative to the 28 days cured uncarbonated concretes, the NS and NSL mixes present a comparable chloride permeability after 28 days of accelerated carbonation, with values comparable to those reported for the NS 28 days cured uncarbonated concrete. The NS2L concrete mix exhibited a much higher chloride migration coefficient upon 28 days of accelerated carbonation than NS and NSL, but the value remains comparable to that of NS2L 28 days cured uncarbonated concrete. An extended accelerated carbonation exposure (100 days) led to an increase in the chloride's migration coefficient of the binary and ternary concretes, reporting values lower or comparable to those of the NS2L 28 days cured uncarbonated concrete. Overall, these marginal increases are also significantly lower when compared to the chloride permeability of 28 days cured CEM I.

The results indicate that binary and ternary concretes containing slag with or without limestone addition, present an excellent chloride permeability performance compared to CEM I even when carbonated. Considering the differences in the age of the carbonated concretes (28 days curing plus 14 days of preconditioning plus carbonation exposure duration) and that of the 28 days uncarbonated concretes, as well as the differences in the RH of carbonation exposure vs curing, it is difficult to attribute the differences in the chloride migration coefficient to specific phenomena. However, differences in the degree of hydration (which is influenced by age as well as by saturation of the specimens), the phase assemblage alteration in the carbonated region and pore structure evolution in the uncarbonated region are the dominant factors influencing the concrete's performance of the different types of cement used post-carbonation.

2.5. Conclusions

Based on the experimental findings on the influence of carbonation on the mechanical and transport properties of concrete made with CEM I, binary cement with 50 wt.% GGBFS, ternary cements with GGBFS plus 10 wt.% limestone and GGBFS with 20 wt.% limestone corresponding to N, NS, NSL and NS2L, respectively, the following deductions can be made:

1. CEM I concrete exhibited high resistance to carbonation relative to the GGBFS-containing concrete, with or without limestone, at all durations of natural or accelerated carbonation exposure. Meanwhile, binary slags and ternary slag concrete exhibited comparable carbonation resistance, suggesting that the addition of limestone has a negligible effect on the progression of the carbonation depth at a similar replacement level to high-volume binary slag concrete.
2. A good correlation between natural and accelerated carbonation coefficients was identified for all the concretes evaluated so that predicted natural carbonation values are similar to those experimentally determined from 1-year natural exposure. Applying the equation correlating natural and accelerated carbonation, carbonation depth predictions indicate that slag containing concrete mixes, with or without limestone addition, are suitable for applications requiring 50 or 100 years of service life, when benchmarked with cover depth recommendations of the BS 8500–1:2023 standard.
3. The residual compressive strength of all carbonated concrete mixes after 100 days of natural and accelerated CO_2 exposure demonstrates that N, NS and NSL continue gaining strength, while NS2L exhibited a decrease in strength. However, the lowest post-carbonation strength of NS2L is still higher than the concrete design strength class. This indicates that the continuous hydration of the binder, despite the moderate RH (57 %) adopted for natural or accelerated carbonation exposure, counteracts the adverse microstructural changes induced by the carbonation reactions.
4. The shrinkage of concretes exposed to ambient conditions is lower in concretes made with composite cements compared to CEM I. While a similar trend was observed under accelerated carbonation, marginal differences in dimensional stability were observed in the ternary mixes. Nonetheless, higher carbonation-affected depths did not induce a significant increase in shrinkage strains in NS, NSL and NS2L relative to CEM I under accelerated carbonation exposure.

Further studies for decoupling the contributions of carbonation, chemical and/or drying shrinkage are necessary to understand how these combined phenomena will influence the long-term dimensional stability in low-clinker composite concrete.

5. Water absorption properties of partially carbonated concretes showed that accelerated carbonation resulted in a reduction of the initial sorptivity coefficients of CEM I. Concrete made with composite slag cements present comparable sorptivity coefficients when exposed to natural or accelerated carbonation. In addition, there is no marked change in the total porosity of the samples neither at early nor at later exposure times, independent of the exposure condition adopted (natural vs accelerated). This indicates that carbonation is inducing changes in the pore size distribution of the materials evaluated but not changes in the total porosity. This is consistent with the compressive strength recorded for carbonated samples, where residual strength was not reduced below the design strength, even for concrete NS2L with the highest carbonation depth.
6. Replacing the GGBFS in blended cements with 10 or 20 wt% limestone addition does not compromise their chloride resistance when both binary and ternary forms are subjected to similar carbonation exposure conditions. Further studies should focus on determining changes in transport properties and chloride penetration resistance in long-term natural carbonated composite concrete.
7. For the testing conditions adopted in this study and for the materials evaluated, no clear correlation was identified between compressive strength, porosity, bulk conductivity, water sorption coefficient and carbonation rate. This suggests that none of those parameters can be used independently to infer the potential longevity of slag-based concrete upon carbonation. This warrants more studies exploring the performance of carbonated cover in reinforced concrete to understand their durability as the existing relationship between microstructure-performance relationship may be fully applicable to carbonated concrete, which is the likely scenario when the materials is in-service.

Overall, it is demonstrated that the partial replacement of GGBFS for up to 20 wt% limestone has no detrimental impact on the carbonation performance of ternary blended concrete mixes. As GGBFS availability in some regions is limited, the use of limestone Portland cement in the form of PLC or CEM II L, along with GGBFS, is increasing globally. Ternary cements are a technically feasible solution for producing concrete with comparable or better durability performance to CEM I or binary slag concretes. Although the higher carbonation depth rates recorded for binary or ternary slag-containing concrete often impair the long-term performance of these materials, carbonation does not induce significant changes in the water or chloride permeability of those concretes to the levels of CEM I concrete. This suggests that carbonation depths, or carbonation coefficient values alone, are not good indicators of the potential long-term durability performance of binary and ternary GGBFS containing concretes when other aggressive agents are present in the in-service environment.

CRediT authorship contribution statement

Moro Sabtiwu: Writing – review & editing, Writing – original draft, Methodology, Investigation, Formal analysis, Data curation, Conceptualization. **Yuvaraj Dhandapani:** Writing – review & editing, Supervision, Methodology, Formal analysis, Conceptualization. **Michal Drewniok:** Writing – review & editing, Supervision. **Samuel Adu-Amankwah:** Writing – review & editing, Supervision. **Susan A. Bernal:** Writing – review & editing, Supervision, Resources, Project administration, Methodology, Funding acquisition, Conceptualization.

Declaration of competing interest

The authors declare the following financial interests/personal relationships which may be considered as potential competing interests: Moro Sabtiwu reports financial support for his PhD studies provided by National Highways Limited. The other co-authors declare that they have no known competing financial interests or personal relationships that could have appeared to influence the work reported in this paper.

Acknowledgements

The PhD research of M. Sabtiwu was sponsored by the UK Engineering and Physical Sciences Research Council (EPSRC) via a CASE PhD studentship co-sponsored by National Highways. Participation of S.A. Bernal in this study was sponsored by the Engineering and Physical Sciences Research Council (EPSRC) via the Early Career Fellowship EP/R001642/1.

Data availability

The data of this study is available in the University of Leeds Research Data Repository accessible in the following link - https://doi.org/10.5518/1708.

References

[1] M. Auroy, S. Poyet, P. Le Bescop, J.-M. Torrenti, T. Charpentier, M. Moskura, X. Bourbon, Impact of carbonation on unsaturated water transport properties of cement-based materials, Cement Concr. Res. 74 (2015) 44–58.
[2] O. Wowra, Effects of carbonation to microstructure and pore solution. International RILEM Workshop on Frost Resistance of Concrete, RILEM Publications SARL, 2002, pp. 61–68.
[3] Z. Shi, B. Lothenbach, M.R. Geiker, J. Kaufmann, A. Leemann, S. Ferreiro, J. Skibsted, Experimental studies and thermodynamic modeling of the carbonation of Portland cement, metakaolin and limestone mortars, Cement Concr. Res. 88 (2016) 60–72.
[4] S. Adu-Amankwah, S. Rahmon, L. Black, From composition to the microstructure and durability of limestone ternary blended cements: a systematic review, Adv. Cement Res. 34 (5) (2022) 206–224.
[5] S. Adu-Amankwah, M. Zajac, C. Stabler, B. Lothenbach, L. Black, Influence of limestone on the hydration of ternary slag cements, Cement Concr. Res. 100 (2017) 96–109.
[6] Y. Dhandapani, M. Santhanam, G. Kaladharan, S. Ramanathan, Towards ternary binders involving limestone additions — a review, Cement Concr. Res. 143 (2021) 106396.
[7] Y. Dhandapani, T. Sakthivel, M. Santhanam, R. Gettu, R.G. Pillai, Mechanical properties and durability performance of concretes with limestone calcined clay cement (LC3), Cement Concr. Res. 107 (2018) 136–151.
[8] M. Zajac, J. Skocek, S. Adu-Amankwah, L. Black, M. Ben Haha, Impact of microstructure on the performance of composite cements: why higher total porosity can result in higher strength, Cement Concr. Compos. 90 (2018) 178–192.
[9] Y. Dhandapani, M. Santhanam, Assessment of pore structure evolution in the limestone calcined clay cementitious system and its implications for performance, Cement Concr. Compos. 84 (2017) 36–47.
[10] Y. Dhandapani, M. Santhanam, Investigation on the microstructure-related characteristics to elucidate performance of composite cement with limestone-calcined clay combination, Cement Concr. Res. 129 (2020) 105959.
[11] S. Adu-Amankwah, M. Zajac, J. Skocek, M. Ben Haha, L. Black, Relationship between cement composition and the freeze–thaw resistance of concretes, Adv. Cement Res. 30 (8) (2018) 387–397.
[12] A. Leemann, F. Moro, Carbonation of concrete: the role of CO_2 concentration, relative humidity and CO_2 buffer capacity, Mater. Struct. 50 (1) (2017) 30.
[13] A. Leemann, P. Nygaard, J. Kaufmann, R. Loser, Relation between carbonation resistance, mix design and exposure of mortar and concrete, Cement Concr. Compos. 62 (2015) 33–43.
[14] F. Lollini, E. Redaelli, Carbonation of blended cement concretes after 12 years of natural exposure, Constr. Build. Mater. 276 (2021) 122122.
[15] P. Sulapha, S. Wong, T. Wee, S. Swaddiwudhipong, Carbonation of concrete containing mineral admixtures, J. Mater. Civ. Eng. 15 (2) (2003) 134–143.
[16] V. Shah, S. Bishnoi, Carbonation resistance of cements containing supplementary cementitious materials and its relation to various parameters of concrete, Constr. Build. Mater. 178 (2018) 219–232.
[17] I. Elkhaldi, E. Roziere, G. Villain, A. Loukili, Effect of accelerated carbonation on electrical resistivity and microstructure of clinker-slag-limestone cement based concretes, Mater. Struct. 57 (2024) 17.
[18] W. Zhang, R. Gao, X. Sha, G. Liu, X.-Y. Wang, R.-S. Lin, Y. Tong, Strength development and thermal stability analysis of carbonation-cured red mud-based cementitious materials, Constr. Build. Mater. 470 (2025) 140724.
[19] T. Proske, M. Rezvani, S. Palm, C. Müller, C.-A. Graubner, Concretes made of efficient multi-composite cements with slag and limestone, Cement Concr. Compos. 89 (2018) 107–119.

[20] U. Angst, F. Moro, M. Geiker, S. Kessler, H. Beushausen, C. Andrade, J. Lahdensivu, A. Köliö, K.-i. Imamoto, S. von Greve-Dierfeld, M. Serdar, Corrosion of steel in carbonated concrete: mechanisms, practical experience, and research Priorities–A critical review by RILEM TC 281-CCC, RILEM Technical Letters 5 (2020) 85–100.
[21] BSI, BS 8500-1: 2015+ A2: 2019. Concrete, Complementary British Standard to BS EN 206. Method of Specifying and Guidance for the Specifier, British Standards Institution, London, 2019.
[22] BS 8500-1. Concrete, Complementary British Standard to BS EN 206. Method of Specifying and Guidance for the Specifier, British Standards Institution, London, 2023.
[23] BS 8500-2. Concrete, Complementary British Standard to BS EN 206. Specification for Constituent Materials and Concrete, British Standards Institute, London, 2023.
[24] BS EN 197-5, Portland-Composite Cement CEM II/C-M and Composite Cement CEM VI, British Standards Institute, London, 2021.
[25] M. Hren, V. Bokan Bosiljkov, A. Legat, Effects of blended cements and carbonation on chloride-induced corrosion propagation, Cement Concr. Res. 145 (2021) 106458.
[26] K. Li, Y. Zhang, S. Wang, J. Zeng, Impact of carbonation on the chloride diffusivity in concrete: experiment, analysis and application, Mater. Struct. 51 (6) (2018) 164.
[27] M. Sabtiwu, Y. Dhandapani, M. Drewniok, S. Adu-Amankwah, S.A. Bernal, Influence of limestone addition on the engineering and durability performance of Portland-blastfurnace slag blended concretes, Constr. Build. Mater. 489 (2025) 142282.
[28] BS 7979, Specification for Limestone Fines for Use with Portland Cement, British Standards Institute, London, 2016.
[29] S. Adu-Amankwah, L. Black, J. Skocek, M. Haha Ben, M. Zajac, Effect of sulfate additions on hydration and performance of ternary slag-limestone composite cements, Constr. Build. Mater. 164 (2018).
[30] BS EN 206:2013+A2. Concrete — Specification, Performance, Production and Conformity, British Standards Institute, London, 2021.
[31] BS EN 12390-2, Testing Hardened Concrete. Making and Curing Specimens for Strength Tests, British Standards Institution, London, 2019.
[32] BS EN 12350-2, Testing Fresh Concrete. Slump-test, British Standards Institution, London, 2019.
[33] BS EN 12350-5. Testing Fresh Concrete. Flow Table Test, British Standard Institute, London, 2019.
[34] BS EN 12350-7, Testing Fresh Concrete: Air content–pressure Methods, British Standards Institution, London, 2019.
[35] BS EN 12350-6, Testing Fresh Concrete. Density, British Standards Institution, London, 2019.
[36] BS EN 12390-12, Determination of the Carbonation Resistance of Concrete — Accelerated Carbonation Method, British Standards Institution, London, 2020.
[37] S.A. Bernal, Y. Dhandapani, Y. Elakneswaran, G.J.G. Gluth, E. Gruyaert, M.C. G. Juenger, B. Lothenbach, K.A. Olonade, M. Sakoparnig, Z. Shi, C. Thiel, P. Van den Heede, H. Vanoutrive, S. von Greve-Dierfeld, N. De Belie, J.L. Provis, Report of RILEM TC 281-CCC: a critical review of the standardised testing methods to determine carbonation resistance of concrete, Mater. Struct. 57 (2024) 173.
[38] https://gbr.sika.com/en/distribution/74493/priming/sika-primer-mb.html. (Accessed 23 May 2025).
[39] BS EN 13057, Products and systems for the protection and repair of concrete structures. test methods, determination of resistance of capillary absorption, British Standards Institute,, London, 2002.
[40] BS 1881-208, Recommendations for the Determination of the Initial Surface Absorption of Concrete, British Standards Institution, London, 1996.
[41] ASTM C 1760, Standard Test Method for Bulk Electrical Conductivity of Hardened Concrete, 2012.
[42] Nordtest NTBuild 492, Concrete, Mortar, Cement Based Repair Materials: Chloride Migration Coefficient from Non-steady State Migration Experiments, 1999.
[43] BS EN 12390-3. Testing hardened concrete: compressive strength of test specimens, British Standard Institute, London, 2019.
[44] BS EN 12390-12. Determination of the Carbonation Resistance of Concrete — Accelerated Carbonation Method, London, UK, 2020.
[45] K. Sisomphon, L. Franke, Carbonation rates of concretes containing high volume of pozzolanic materials, Cement Concr. Res. 37 (12) (2007) 1647–1653.
[46] Q. Huy Vu, G. Pham, A. Chonier, E. Brouard, S. Rathnarajan, R. Pillai, R. Gettu, M. Santhanam, F. Aguayo, K.J. Folliard, M.D. Thomas, T. Moffat, C. Shi, A. Sarnot, Impact of different climates on the resistance of concrete to natural carbonation, Constr. Build. Mater. 216 (2019) 450–467.
[47] C.D. Atiş, C. Bilim, Wet and dry cured compressive strength of concrete containing ground granulated blast-furnace slag, Build. Environ. 42 (8) (2007) 3060–3065.
[48] S.N. Lim, T.H. Wee, Autogenous shrinkage of ground-granulated blast-furnace slag concrete, Mater. J. 97 (5) (2000) 587–593.
[49] M. Bouasker, N.E.H. Khalifa, P. Mounanga, N. Ben Kahla, Early-age deformation and autogenous cracking risk of slag–limestone filler-cement blended binders, Constr. Build. Mater. 55 (2014) 158–167.
[50] A.M. Neville, Properties of Concrete, Longman London, 1995, pp. 426–445.
[51] M. Rezvani, T. Proske, C.-A. Graubner, Modelling the drying shrinkage of concrete made with limestone-rich cements, Cement Concr. Res. 115 (2019) 160–175.
[52] A.K.H. Kwan, M. McKinley, J.-J. Chen, Adding limestone fines as cement paste replacement to reduce shrinkage of concrete, Mag. Concr. Res. 65 (15) (2013) 942–950.
[53] Z. Liu, P. Van den Heede, C. Zhang, X. Shi, L. Wang, J. Li, Y. Yao, B. Lothenbach, N. De Belie, Carbonation of blast furnace slag concrete at different CO_2 concentrations: carbonation rate, phase assemblage, microstructure and thermodynamic modelling, Cement Concr. Res. 169 (2023) 107161.
[54] C. Hall, Water sorptivity of mortars and concretes: a review, Mag. Concr. Res. 41 (147) (1989) 51–61.
[55] J. Castro, D. Bentz, J. Weiss, Effect of sample conditioning on the water absorption of concrete, Cement Concr. Compos. 33 (8) (2011) 805–813.
[56] C.A. Rigo da Silva, R.J. Pedrosa Reis, F. Soares Lameiras, W.L. Vasconcelos, Carbonation-related microstructural changesin long-term durability concrete, Mater. Res. 5 (2002).
[57] W.P.S. Dias, Reduction of concrete sorptivity with age through carbonation, Cement Concr. Res. 30 (8) (2000) 1255–1261.
[58] J.J. Chen, A.K.H. Kwan, Y. Jiang, Adding limestone fines as cement paste replacement to reduce water permeability and sorptivity of concrete, Constr. Build. Mater. 56 (2014) 87–93.
[59] V. Baroghel-Bouny, Which toolkit for durability evaluation as regards chloride ingress into concrete? Part II: development of a performance approach based on durability indicators and monitoring parameters, in: Third International RILEM Workshop on Testing and Modeling Chloride Ingress into Concrete, 2024, pp. 137–163.
[60] A. Lübeck, A.L.G. Gastaldini, D.S. Barin, H.C. Siqueira, Compressive strength and electrical properties of concrete with white Portland cement and blast-furnace slag, Cement Concr. Compos. 34 (3) (2012) 392–399.
[61] X. Ke, S.A. Bernal, J.L. Provis, Uptake of chloride and carbonate by Mg-Al and Ca-Al layered double hydroxides in simulated pore solutions of alkali-activated slag cement, Cement Concr. Res. 100 (2017) 1–13.
[62] E.P. Nielsen, D. Herfort, M.R. Geiker, Binding of chloride and alkalis in Portland cement systems, Cement Concr. Res. 35 (1) (2005) 117–123.
[63] D.G. Mapa, H. Zhu, F. Nosouhian, N. Shanahan, K.A. Riding, A. Zayed, Chloride binding and diffusion of slag blended concrete mixtures, Constr. Build. Mater. 388 (2023) 131584.
[64] Q. Yuan, C. Shi, G. De Schutter, K. Audenaert, D.J.C. Deng, Chloride binding of cement-based materials subjected to external chloride environment – a review, Constr. Build. Mater. 23 (1) (2009) 1–13.